

EUROPEAN ORGANIZATION FOR NUCLEAR RESEARCH (CERN)



CERN-PH-EP-2014-173
 LHCb-PAPER-2014-034
 22 July 2014

Evidence for CP violation in $B^+ \rightarrow p\bar{p}K^+$ decays

The LHCb collaboration[†]

Abstract

Three-body $B^+ \rightarrow p\bar{p}K^+$ and $B^+ \rightarrow p\bar{p}\pi^+$ decays are studied using a data sample corresponding to an integrated luminosity of 3.0 fb^{-1} collected by the LHCb experiment in proton-proton collisions at center-of-mass energies of 7 and 8 TeV. Evidence of CP violation in the $B^+ \rightarrow p\bar{p}K^+$ decay is found in regions of the phase space, representing the first measurement of this kind for a final state containing baryons. Measurements of the forward-backward asymmetry of the light meson in the $p\bar{p}$ rest frame yield $A_{\text{FB}}(p\bar{p}K^+, m_{p\bar{p}} < 2.85 \text{ GeV}/c^2) = 0.495 \pm 0.012 \text{ (stat)} \pm 0.007 \text{ (syst)}$ and $A_{\text{FB}}(p\bar{p}\pi^+, m_{p\bar{p}} < 2.85 \text{ GeV}/c^2) = -0.409 \pm 0.033 \text{ (stat)} \pm 0.006 \text{ (syst)}$. In addition, the branching fraction of the decay $B^+ \rightarrow \bar{\Lambda}(1520)p$ is measured to be $\mathcal{B}(B^+ \rightarrow \bar{\Lambda}(1520)p) = (3.15 \pm 0.48 \text{ (stat)} \pm 0.07 \text{ (syst)} \pm 0.26 \text{ (BF)}) \times 10^{-7}$, where BF denotes the uncertainty on secondary branching fractions.

Submitted to Phys. Rev. Lett.

© CERN on behalf of the LHCb collaboration, license CC-BY-4.0.

[†]Authors are listed at the end of this article.

Direct CP violation can appear as a rate asymmetry in the decay of a particle and its CP conjugate, and can be observed when at least two amplitudes, carrying different weak and strong phases, contribute to the final state. For B mesons, it was observed for the first time in two-body $B^0 \rightarrow K^+ \pi^-$ decays [1, 2]. The weak phases are sensitive to physics beyond the Standard Model that may appear at a high energy scale, and their extraction requires a determination of the relative strong phases. Three-body decays are an excellent laboratory for studying strong phases of interfering amplitudes. In particular, charmless decays of B^+ mesons, $B^+ \rightarrow K^+ \pi^- \pi^+$, $B^+ \rightarrow K^+ K^- K^+$, $B^+ \rightarrow \pi^+ \pi^- \pi^+$, $B^+ \rightarrow K^+ K^- \pi^+$ have been investigated recently [3–5]¹. Similar studies have been conducted for the baryonic final states $B^+ \rightarrow p\bar{p}K^+$ and $B^+ \rightarrow p\bar{p}\pi^+$ [6]. In the $B^+ \rightarrow h^+ h^- h^+$ decays ($h = \pi$ or K throughout this Letter), large asymmetries, not necessarily associated to resonances, have been observed in the low $K^+ K^-$ and $\pi^+ \pi^-$ mass regions. These observations suggest that rescattering between $\pi^+ \pi^-$ and $K^+ K^-$ pairs may play an important role in the generation of the strong phase difference needed for CP violation to occur [7]. The $B^+ \rightarrow p\bar{p}h^+$ decays, although sharing the same quark-level diagrams, may exhibit different behavior due to the baryonic nature of two out of the three final-state particles.

This Letter reports the first evidence for CP violation in charmless $B^+ \rightarrow p\bar{p}K^+$ decays. These decays are studied in the region with invariant mass $m_{p\bar{p}} < 2.85 \text{ GeV}/c^2$, below the charmonium resonances threshold. In addition, a more accurate measurement of the branching fraction of the decay $B^+ \rightarrow \bar{\Lambda}(1520)p$ is performed, using the reconstruction of $\bar{\Lambda}(1520) \rightarrow K^+ \bar{p}$ decays, and improved determinations of the spectra and angular asymmetries are also reported. The mode $B^+ \rightarrow J/\psi(\rightarrow p\bar{p})K^+$ serves as a control channel. The data used have been collected with the LHCb detector and correspond to 1.0 and 2.0 fb^{-1} of integrated luminosity at 7 and 8 TeV center-of-mass energies in pp collisions, respectively. The data samples are analyzed separately and the results are averaged.

The LHCb detector is a single-arm forward spectrometer covering the pseudorapidity range $2 < \eta < 5$, described in detail in Ref. [8]. The detector allows for the reconstruction of both charged and neutral particles. For this analysis, the ring-imaging Cherenkov (RICH) detectors [9], distinguishing pions, kaons and protons, are particularly important.

The analysis uses simulated events generated by PYTHIA 8.1 [10] with a specific LHCb configuration [11]. Decays of hadronic particles are described by EVTGEN [12] in which final state radiation is generated using PHOTOS [13]. The interaction of the generated particles with the detector and its response are implemented using the GEANT4 toolkit [14] as described in Ref. [15]. Nonresonant $B^+ \rightarrow p\bar{p}h^+$ events are simulated, uniformly distributed in phase space, to study the variation of efficiencies across the Dalitz [16] plane, as well as resonant modes such as $B^+ \rightarrow J/\psi(\rightarrow p\bar{p})K^+$, $B^+ \rightarrow \eta_c(\rightarrow p\bar{p})K^+$, $B^+ \rightarrow \psi(2S)(\rightarrow p\bar{p})K^+$, $B^+ \rightarrow \bar{\Lambda}(1520)(\rightarrow K^+ \bar{p})p$, and $B^+ \rightarrow J/\psi(\rightarrow p\bar{p})\pi^+$.

Three charged particles are combined to form $B^+ \rightarrow p\bar{p}h^+$ decay candidates. The discrimination of signal from background is done through a multivariate analysis using a boosted decision tree (BDT) classifier [17]. Input quantities include kinematical and

¹Throughout the Letter, the inclusion of charge conjugate processes is implied, except in the definition of CP asymmetries.

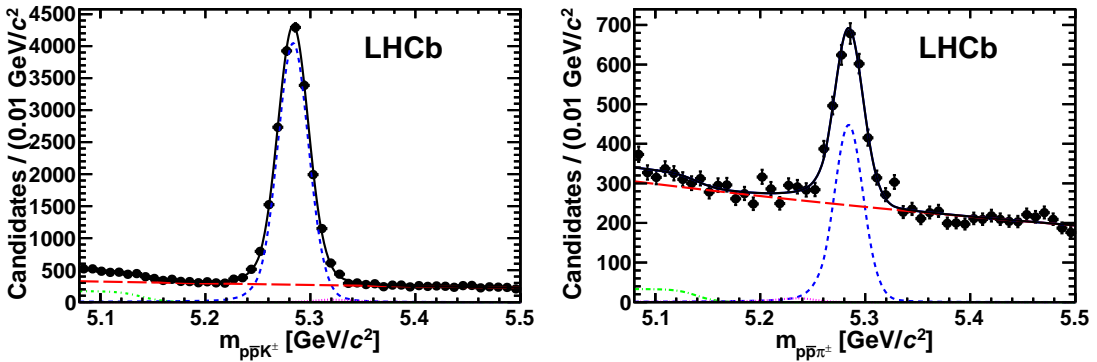


Figure 1: Invariant mass distributions of (left) $p\bar{p}K^+$ and (right) $p\bar{p}\pi^+$ candidates. The points with error bars represent data. The solid black line represents the total fit function. The components are represented by blue dashed (signal), purple dotted (cross-feed), red long-dashed (combinatorial background) and green dashed-dotted (partially reconstructed background) curves.

topological variables related to the B^+ candidates and the individual tracks. The momentum, vertex and flight distance of the B^+ candidate are exploited, and track fit quality criteria, impact parameter and momentum information of final-state particles are also used. The BDT is trained using simulated signal events, and events in the high sideband of the $p\bar{p}h^+$ invariant mass ($5.4 < m(p\bar{p}h^+) < 5.5 \text{ GeV}/c^2$), which represent the background. Tight particle identification (PID) requirements are applied to reduce the combinatorial background and suppress the cross-feed between $p\bar{p}K^+$ and $p\bar{p}\pi^+$. The PID efficiencies are derived from calibration data samples of kinematically identified pions, kaons and protons originating from the decays $D^{*+} \rightarrow D^0(\rightarrow K^-\pi^+)\pi^+$ and $\Lambda \rightarrow p\pi^-$.

Signal and background yields are extracted using unbinned extended maximum likelihood fits to the invariant mass distribution of the $p\bar{p}h^+$ combinations. The $B^+ \rightarrow p\bar{p}K^+$ signal is modeled by the sum of two Crystal Ball functions [18], for which the common mean and core width are allowed to float in the fit. Beside the signal component, the fit includes the parameterizations of the combinatorial background and partially reconstructed $B \rightarrow p\bar{p}K^*$ decays, where a pion from the K^* decay is not reconstructed, resulting in a $p\bar{p}K$ invariant mass below the nominal B mass. An asymmetric Gaussian function with power-law tails is used to model a possible $p\bar{p}\pi^+$ cross-feed component, where the pion is misidentified as a kaon. This contribution is found to be small.

The fit to the $B^+ \rightarrow p\bar{p}\pi^+$ decay uses similar parameterizations for the signal, combinatorial background, $p\bar{p}K^+$ cross-feed and partially reconstructed background from $B \rightarrow p\bar{p}\rho$ decays (with a missing pion from the ρ decay). The cross-feed is found to be negligible.

The $B^+ \rightarrow p\bar{p}h^+$ invariant mass spectra are shown in Fig. 1. The signal yields obtained from the fits are $N(p\bar{p}K^\pm) = 18\,721 \pm 142$ and $N(p\bar{p}\pi^\pm) = 1988 \pm 74$, where the uncertainties are statistical only.

The distribution of events in the Dalitz plane, defined by $(m_{p\bar{p}}^2, m_{hp}^2)$ where hp denotes the neutral combinations h^-p and $h^+\bar{p}$, is examined. From the fits to the B^+ candidate

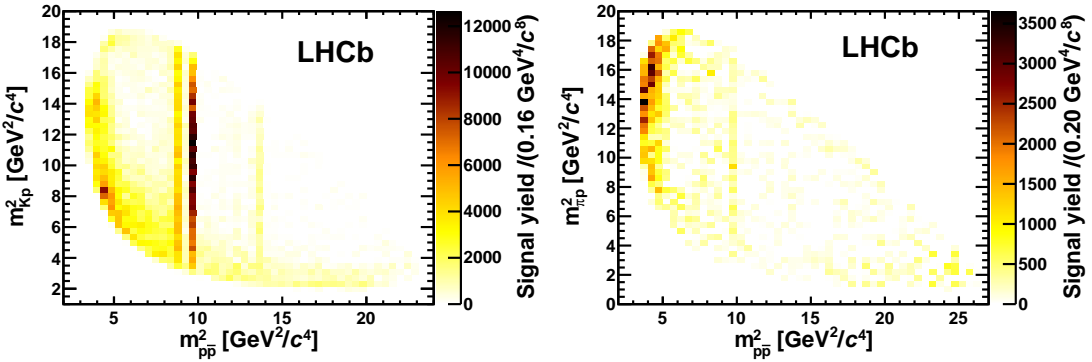


Figure 2: Background-subtracted and acceptance-corrected Dalitz-plot distributions for (left) $B^+ \rightarrow p\bar{p}K^+$ and (right) $B^+ \rightarrow p\bar{p}\pi^+$.

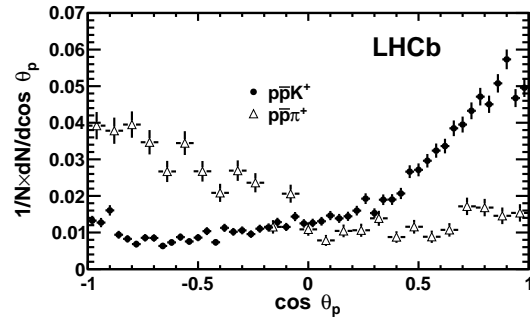


Figure 3: Background-subtracted and acceptance-corrected normalized distributions of $\cos \theta_p$ for $B^+ \rightarrow p\bar{p}K^+$ and $B^+ \rightarrow p\bar{p}\pi^+$ decays, for $m_{p\bar{p}} < 2.85 \text{ GeV}/c^2$. The data points are shown with their total uncertainties.

invariant mass, shown in Fig. 1, signal weights are calculated with the *sPlot* technique [19]. These weights are corrected for trigger, reconstruction and selection efficiencies, which are estimated with simulated samples and calibration data. The Dalitz-plot variables are calculated constraining the $p\bar{p}h^+$ invariant mass to the known B^+ meson mass [20, 21]. Figure 2 shows the Dalitz distributions of the $B^+ \rightarrow p\bar{p}h^+$ events. Similarly to the results reported in Ref. [6, 22], clear signals of J/ψ , η_c and $\psi(2S)$ resonances are observed, while $B^+ \rightarrow p\bar{p}K^+$ and $B^+ \rightarrow p\bar{p}\pi^+$ non-charmonium events both accumulate near the $p\bar{p}$ threshold. However, $B^+ \rightarrow p\bar{p}K^+$ events preferentially occupy the region with low Kp invariant mass while $B^+ \rightarrow p\bar{p}\pi^+$ events populate the region with large πp invariant mass. This difference in the Dalitz distribution can also be observed as a difference in the distribution of the helicity angle θ_p of the $p\bar{p}$ system, defined as the angle between the charged meson h and the oppositely charged baryon in the rest frame of the $p\bar{p}$ system. The distributions of $\cos(\theta_p)$ are depicted in Fig. 3.

Data and simulation are used to assign systematic uncertainties, accounting for the

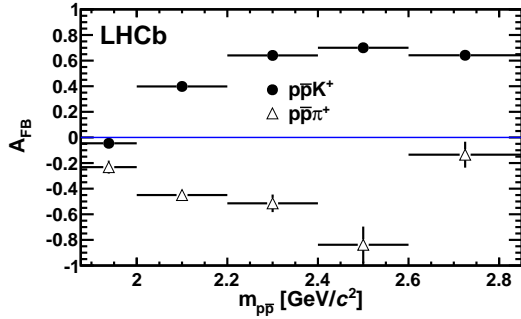


Figure 4: Forward-backward asymmetry in bins of $m_{pp\bar{p}}$ for $B^+ \rightarrow p\bar{p}K^+$ and $B^+ \rightarrow p\bar{p}\pi^+$ decays. The data points are shown with their total uncertainties.

PID correction and fit model, to the angular and charge asymmetries, and to the relative branching fractions. The systematic uncertainty associated to the PID correction cancels in the asymmetry measurements.

The forward-backward asymmetry is measured as

$$A_{FB} = \frac{N_{\text{pos}} - N_{\text{neg}}}{N_{\text{pos}} + N_{\text{neg}}}, \quad (1)$$

where N_{pos} (N_{neg}) is the efficiency-corrected yield for $\cos \theta_p > 0$ ($\cos \theta_p < 0$). The obtained asymmetries are $A_{FB}(p\bar{p}K^+, m_{pp\bar{p}} < 2.85 \text{ GeV}/c^2) = 0.495 \pm 0.012 \text{ (stat)} \pm 0.007 \text{ (syst)}$ and $A_{FB}(p\bar{p}\pi^+, m_{pp\bar{p}} < 2.85 \text{ GeV}/c^2) = -0.409 \pm 0.033 \text{ (stat)} \pm 0.006 \text{ (syst)}$, where the systematic uncertainty is due to the ratio of average efficiencies in the regions $\cos \theta_p > 0$ and $\cos \theta_p < 0$. As reported in previous studies [6, 23], the value for $B^+ \rightarrow p\bar{p}K^+$ contradicts the short-range analysis expectation [24]. The values of A_{FB} in bins of $m_{pp\bar{p}}$ are shown in Fig. 4; in both cases, they depend strongly on $m_{pp\bar{p}}$.

The yields of the decays $B^+ \rightarrow p\bar{p}h^+$ in the region $m_{pp\bar{p}} < 2.85 \text{ GeV}/c^2$ are obtained in the same way as for the integrated signals. Those of the resonant modes are extracted through two-dimensional extended unbinned maximum likelihood fits to invariant mass distributions of $p\bar{p}h^+$ and $p\bar{p}$ or $K^+\bar{p}$, using the same signal and background models for $m_{pp\bar{p}}$ or $m_{K^+\bar{p}}$ as in Ref. [6]. The results are shown in Table 1. The branching fractions of the decays $B^+ \rightarrow \bar{\Lambda}(1520)(\rightarrow K^+\bar{p})p$ and $B^+ \rightarrow p\bar{p}\pi^+, m_{pp\bar{p}} < 2.85 \text{ GeV}/c^2$ are measured relative to the J/ψ modes as

$$\begin{aligned} \frac{\mathcal{B}(B^+ \rightarrow \bar{\Lambda}(1520)(\rightarrow K^+\bar{p})p)}{\mathcal{B}(B^+ \rightarrow J/\psi(\rightarrow p\bar{p})K^+)} &= 0.033 \pm 0.005 \text{ (stat)} \pm 0.007 \text{ (syst)}, \\ \frac{\mathcal{B}(B^+ \rightarrow p\bar{p}\pi^+, m_{pp\bar{p}} < 2.85 \text{ GeV}/c^2)}{\mathcal{B}(B^+ \rightarrow J/\psi(\rightarrow p\bar{p})\pi^+)} &= 12.0 \pm 1.2 \text{ (stat)} \pm 0.3 \text{ (syst)}. \end{aligned}$$

The systematic uncertainties also include contributions from the background model. Using $\mathcal{B}(B^+ \rightarrow J/\psi K^+) = (1.016 \pm 0.033) \times 10^{-3}$, $\mathcal{B}(B^+ \rightarrow J/\psi \pi^+) = (4.1 \pm 0.4) \times 10^{-5}$,

Table 1: Event yields and selection efficiency for $B^+ \rightarrow p\bar{p}K^+$ and $B^+ \rightarrow p\bar{p}\pi^+$ final states.

Mode	Yield	Efficiency (%)
$B^+ \rightarrow J/\psi(\rightarrow p\bar{p})K^+$	4260 ± 67	1.55 ± 0.02
$B^+ \rightarrow \eta_c(\rightarrow p\bar{p})K^+$	2182 ± 64	1.47 ± 0.02
$B^+ \rightarrow \psi(2S)(\rightarrow p\bar{p})K^+$	368 ± 20	1.59 ± 0.02
$B^+ \rightarrow \bar{\Lambda}(1520)(\rightarrow K^+\bar{p})p$	128 ± 20	1.39 ± 0.01
$B^+ \rightarrow p\bar{p}K^+, m_{p\bar{p}} < 2.85 \text{ GeV}/c^2$	8510 ± 104	1.58 ± 0.02
$B^+ \rightarrow J/\psi(\rightarrow p\bar{p})\pi^+$	122 ± 12	1.07 ± 0.01
$B^+ \rightarrow p\bar{p}\pi^+, m_{p\bar{p}} < 2.85 \text{ GeV}/c^2$	1632 ± 64	1.15 ± 0.01

$\mathcal{B}(J/\psi \rightarrow p\bar{p}) = (2.17 \pm 0.07) \times 10^{-3}$ [21], and $\mathcal{B}(\Lambda(1520) \rightarrow K^-p) = 0.234 \pm 0.016$ [25], the branching fractions are measured to be:

$$\begin{aligned} \mathcal{B}(B^+ \rightarrow \bar{\Lambda}(1520)p) &= (3.15 \pm 0.48 \text{ (stat)} \pm 0.07 \text{ (syst)} \pm 0.26 \text{ (BF)}) \times 10^{-7}, \\ \mathcal{B}(B^+ \rightarrow p\bar{p}\pi^+, m_{p\bar{p}} < 2.85 \text{ GeV}/c^2) &= (1.07 \pm 0.11 \text{ (stat)} \pm 0.03 \text{ (syst)} \pm 0.11 \text{ (BF)}) \times 10^{-6}, \end{aligned}$$

where BF denotes the uncertainty on the aforementioned secondary branching fractions. The former measurement supersedes what is reported in Ref. [6].

The raw charge asymmetry is measured from the yields N as

$$A_{\text{raw}} = \frac{N(B^- \rightarrow p\bar{p}h^-) - N(B^+ \rightarrow p\bar{p}h^+)}{N(B^- \rightarrow p\bar{p}h^-) + N(B^+ \rightarrow p\bar{p}h^+)}, \quad (2)$$

and is investigated in the Dalitz plane using signal weights inferred from the fits shown in Fig. 1, for B^- and B^+ samples. This asymmetry includes production and detection asymmetries. The statistics of the $B^\pm \rightarrow p\bar{p}\pi^\pm$ decays is not sufficient to perform such an analysis, so only the $B^\pm \rightarrow p\bar{p}K^\pm$ case is studied. An adaptative binning algorithm is used so that the sum of B^- and B^+ events in each bin is approximately constant. Figure 5 shows the distribution of A_{raw} in the Dalitz plane. A clear pattern is observed near the $p\bar{p}$ threshold where A_{raw} is negative for $m_{Kp}^2 < 10 \text{ GeV}^2/c^4$ and positive for $m_{Kp}^2 > 10 \text{ GeV}^2/c^4$. Figure 6 shows the $m_{p\bar{p}}^2$ projections of $N(B^-) - N(B^+)$ in the regions of interest.

To quantify the effect, unbinned extended maximum likelihood simultaneous fits to B^- and B^+ samples are performed in regions of the Dalitz plane, using the same models as the global fits. The raw asymmetry is corrected for acceptance, by taking into account the small difference in average efficiency due to the B^- and B^+ samples populating differently the Dalitz plane. Physical asymmetries are obtained after acceptance correction ($A_{\text{raw}}^{\text{acc}}$) and accounting for the production $A_{\text{P}}(B^\pm)$ and kaon detection $A_{\text{det}}(K^\pm)$ asymmetries:

$$A_{CP} = A_{\text{raw}}^{\text{acc}} - A_{\text{P}}(B^\pm) - A_{\text{det}}(K^\pm). \quad (3)$$

The decay $B^\pm \rightarrow J/\psi(p\bar{p})K^\pm$, part of the selected sample, is used to determine $A_\Delta = A_{\text{P}}(B^\pm) + A_{\text{det}}(K^\pm)$:

$$A_\Delta = A_{\text{raw}}(B^\pm \rightarrow J/\psi(p\bar{p})K^\pm) - A_{CP}(B^\pm \rightarrow J/\psi K^\pm). \quad (4)$$

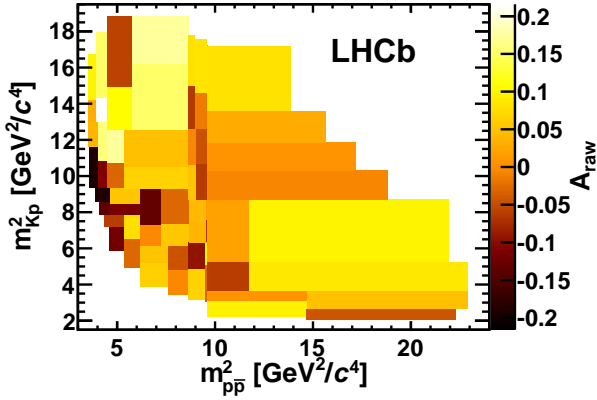


Figure 5: Asymmetries of the number of signal events in bins of the Dalitz-plot variables for $B^\pm \rightarrow p\bar{p}K^\pm$. The number of events in each bin is approximately 300.

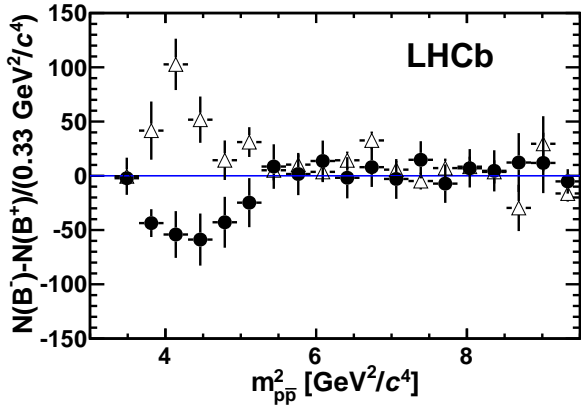


Figure 6: $N(B^-) - N(B^+)$ in bins of $m_{\bar{p}p}^2$ for $m_{Kp}^2 < 10$ GeV $^2/c^4$ (black filled circles) and $m_{Kp}^2 > 10$ GeV $^2/c^4$ (open triangles).

The value $A_{CP}(B^\pm \rightarrow J/\psi K^\pm) = (0.6 \pm 0.4)\%$ is taken from Ref. [26]. When using $A_{\text{raw}}(B^\pm \rightarrow J/\psi(p\bar{p})K^\pm)$, differences in the momentum asymmetry of the $p\bar{p}$ pair between $B^\pm \rightarrow J/\psi(p\bar{p})K^\pm$ and nonresonant $B^\pm \rightarrow p\bar{p}K^\pm$ decays are accounted for. A similar procedure is applied to obtain $A_{CP}(B^\pm \rightarrow \eta_c(p\bar{p})K^\pm)$ and $A_{CP}(B^\pm \rightarrow \psi(2S)(p\bar{p})K^\pm)$. The $B^\pm \rightarrow p\bar{p}\pi^\pm$ decays are also considered in the region $m_{\bar{p}p} < 2.85$ GeV/ c^2 . In this case, the correction also involves the pion detection asymmetry, $A'_\Delta = A_{\text{raw}}(B^\pm \rightarrow J/\psi(p\bar{p})K^\pm) - A_{CP}(B^\pm \rightarrow J/\psi K^\pm) - A_{\text{det}}(K^\pm) + A_{\text{det}}(\pi^\pm)$. The value $A_{\text{det}}(K^\pm) - A_{\text{det}}(\pi^\pm) = (-1.2 \pm 0.1)\%$ is taken from studies of prompt D^+ decays [27]. Table 2 shows the results, including asymmetries of resonant modes. Closer to the $p\bar{p}$ threshold enhancement, $m_{\bar{p}p}^2 < 6$ GeV $^2/c^4$, the asymmetry is found to reach the value -0.066 ± 0.026 (stat) ± 0.004 (syst), for $m_{Kp}^2 < 10$ GeV $^2/c^4$.

Table 2: CP asymmetries for $B^\pm \rightarrow p\bar{p}K^\pm$ and $B^\pm \rightarrow p\bar{p}\pi^\pm$ decays. The systematic uncertainties are dominated by the precision on the measurement $A_{CP}(B^\pm \rightarrow J/\psi K^\pm)$.

Mode/region	A_{CP}
$\eta_c(p\bar{p})K^\pm$	0.040 ± 0.034 (stat) ± 0.004 (syst)
$\psi(2S)(p\bar{p})K^\pm$	0.092 ± 0.058 (stat) ± 0.004 (syst)
$p\bar{p}K^\pm, m_{p\bar{p}} < 2.85 \text{ GeV}/c^2$	0.021 ± 0.020 (stat) ± 0.004 (syst)
$p\bar{p}K^\pm, m_{p\bar{p}} < 2.85 \text{ GeV}/c^2, m_{K_p}^2 < 10 \text{ GeV}^2/c^4$	-0.036 ± 0.023 (stat) ± 0.004 (syst)
$p\bar{p}K^\pm, m_{p\bar{p}} < 2.85 \text{ GeV}/c^2, m_{K_p}^2 > 10 \text{ GeV}^2/c^4$	0.096 ± 0.024 (stat) ± 0.004 (syst)
$p\bar{p}\pi^\pm, m_{p\bar{p}} < 2.85 \text{ GeV}/c^2$	-0.041 ± 0.039 (stat) ± 0.005 (syst)

The systematic uncertainties are estimated by using alternative fit functions and splitting the data sample according to trigger requirements and magnet polarity. The overall systematic uncertainties are dominated by the uncertainty on the $A_{CP}(B^\pm \rightarrow J/\psi K^\pm)$ measurement.

In summary, an interesting sign-inversion pattern of the CP asymmetry appears at low $p\bar{p}$ invariant masses in $B^\pm \rightarrow p\bar{p}K^\pm$ decays. Although this resembles what is observed at low h^+h^- masses in the $B^\pm \rightarrow h^\pm h^+h^-$ decays, the strong phase difference could involve a specific mechanism such as interfering long-range $p\bar{p}$ waves with different angular momenta [24]. In the region $m_{p\bar{p}} < 2.85 \text{ GeV}/c^2, m_{K_p}^2 > 10 \text{ GeV}^2/c^4$, the measured asymmetry is positive with a significance of nearly 4σ , which represents the first evidence of CP violation in b -hadron decays with baryons in the final state. In the region ($m_{p\bar{p}}^2 < 6 \text{ GeV}^2/c^4, m_{K_p}^2 < 10 \text{ GeV}^2/c^4$), the asymmetry is negative with a significance of 2.5σ . The h hadron forward-backward asymmetry in non-charmonium $B^+ \rightarrow p\bar{p}h^+$ decays is measured as $A_{FB}(p\bar{p}K^+, m_{p\bar{p}} < 2.85 \text{ GeV}/c^2) = 0.495 \pm 0.012$ (stat) ± 0.007 (syst) and $A_{FB}(p\bar{p}\pi^+, m_{p\bar{p}} < 2.85 \text{ GeV}/c^2) = -0.409 \pm 0.033$ (stat) ± 0.006 (syst). These asymmetries could be interpreted as being due to the dominance of nonresonant $p\bar{p}$ scattering [24]. Finally, an improved measurement of $\mathcal{B}(B^+ \rightarrow \bar{\Lambda}(1520)p) = (3.15 \pm 0.48 \text{ (stat)} \pm 0.07 \text{ (syst)} \pm 0.26 \text{ (BF)}) \times 10^{-7}$ is obtained.

Acknowledgements

We express our gratitude to our colleagues in the CERN accelerator departments for the excellent performance of the LHC. We thank the technical and administrative staff at the LHCb institutes. We acknowledge support from CERN and from the national agencies: CAPES, CNPq, FAPERJ and FINEP (Brazil); NSFC (China); CNRS/IN2P3 (France); BMBF, DFG, HGF and MPG (Germany); SFI (Ireland); INFN (Italy); FOM and NWO (The Netherlands); MNiSW and NCN (Poland); MEN/IFA (Romania); MinES and FANO (Russia); MinECo (Spain); SNSF and SER (Switzerland); NASU (Ukraine); STFC (United Kingdom); NSF (USA). The Tier1 computing centres are supported by IN2P3 (France),

KIT and BMBF (Germany), INFN (Italy), NWO and SURF (The Netherlands), PIC (Spain), GridPP (United Kingdom). We are indebted to the communities behind the multiple open source software packages on which we depend. We are also thankful for the computing resources and the access to software R&D tools provided by Yandex LLC (Russia). Individual groups or members have received support from EPLANET, Marie Skłodowska-Curie Actions and ERC (European Union), Conseil général de Haute-Savoie, Labex ENIGMASS and OCEVU, Région Auvergne (France), RFBR (Russia), XuntaGal and GENCAT (Spain), Royal Society and Royal Commission for the Exhibition of 1851 (United Kingdom).

References

- [1] BaBar collaboration, B. Aubert *et al.*, *Direct CP violating asymmetry in $B^0 \rightarrow K^+ \pi^-$ decays*, Phys. Rev. Lett. **93** (2004) 131801, [arXiv:hep-ex/0407057](https://arxiv.org/abs/hep-ex/0407057).
- [2] Belle collaboration, Y. Chao *et al.*, *Evidence for direct CP violation in $B^0 \rightarrow K^+ \pi^-$ decays*, Phys. Rev. Lett. **93** (2004) 191802, [arXiv:hep-ex/0408100](https://arxiv.org/abs/hep-ex/0408100).
- [3] LHCb collaboration, R. Aaij *et al.*, *Measurement of CP violation in the phase space of $B^\pm \rightarrow K^\pm \pi^+ \pi^-$ and $B^\pm \rightarrow K^\pm K^+ K^-$ decays*, Phys. Rev. Lett. **111** (2013) 101801, [arXiv:1306.1246](https://arxiv.org/abs/1306.1246).
- [4] LHCb collaboration, R. Aaij *et al.*, *Measurement of CP violation in the phase space of $B^\pm \rightarrow K^+ K^- \pi^\pm$ and $B^\pm \rightarrow \pi^+ \pi^- \pi^\pm$ decays*, Phys. Rev. Lett. **112** (2014) 011801, [arXiv:1310.4740](https://arxiv.org/abs/1310.4740).
- [5] LHCb collaboration, R. Aaij *et al.*, *Measurement of CP violation in the phase space of charmless three-body B^\pm decays*, LHCb-PAPER-2014-044, in preparation.
- [6] LHCb collaboration, R. Aaij *et al.*, *Studies of the decays $B^+ \rightarrow p\bar{p}h^+$ and observation of $B^+ \rightarrow \bar{\Lambda}(1520)p$* , Phys. Rev. **D88** (2013) 052015, [arXiv:1307.6165](https://arxiv.org/abs/1307.6165).
- [7] L. Wolfenstein, *Final state interactions and CP violation in weak decays*, Phys. Rev. **D43** (1991) 151.
- [8] LHCb collaboration, A. A. Alves Jr. *et al.*, *The LHCb detector at the LHC*, JINST **3** (2008) S08005.
- [9] M. Adinolfi *et al.*, *Performance of the LHCb RICH detector at the LHC*, Eur. Phys. J. **C73** (2013) 2431, [arXiv:1211.6759](https://arxiv.org/abs/1211.6759).
- [10] T. Sjöstrand, S. Mrenna, and P. Skands, *A Brief Introduction to PYTHIA 8.1*, Comput. Phys. Comm. **178** (2008) 852, [arXiv:0710.3820](https://arxiv.org/abs/0710.3820).

- [11] I. Belyaev *et al.*, *Handling of the generation of primary events in GAUSS, the LHCb simulation framework*, Nuclear Science Symposium Conference Record (NSS/MIC) **IEEE** (2010) 1155.
- [12] D. J. Lange, *The EvtGen particle decay simulation package*, Nucl. Instrum. Meth. **A462** (2001) 152.
- [13] P. Golonka and Z. Was, *PHOTOS Monte Carlo: a precision tool for QED corrections in Z and W decays*, Eur. Phys. J. **C45** (2006) 97, [arXiv:hep-ph/0506026](https://arxiv.org/abs/hep-ph/0506026).
- [14] Geant4 collaboration, J. Allison *et al.*, *Geant4 developments and applications*, IEEE Trans. Nucl. Sci. **53** (2006) 270; Geant4 collaboration, S. Agostinelli *et al.*, *Geant4: a simulation toolkit*, Nucl. Instrum. Meth. **A506** (2003) 250.
- [15] M. Clemencic *et al.*, *The LHCb simulation application, GAUSS: design, evolution and experience*, J. Phys.: Conf. Ser. **331** (2011) 032023.
- [16] R. H. Dalitz, *On the analysis of τ -meson data and the nature of the τ -meson*, Phil. Mag. **44** (1953) 1068.
- [17] L. Breiman, J. H. Friedman, R. A. Olshen, and C. J. Stone, *Classification and regression trees*, Wadsworth international group, Belmont, California, USA, 1984.
- [18] T. Skwarnicki, *A study of the radiative cascade transitions between the Upsilon-prime and Upsilon resonances*, PhD thesis, Institute of Nuclear Physics, Krakow, 1986, DESY-F31-86-02.
- [19] M. Pivk and F. R. Le Diberder, *sPlot: A statistical tool to unfold data distributions*, Nucl. Instrum. Meth. **A555** (2005) 356, [arXiv:physics/0402083](https://arxiv.org/abs/physics/0402083).
- [20] W. D. Hulsbergen, *Decay chain fitting with a Kalman filter*, Nucl. Instrum. Meth. **A552** (2005) 566, [arXiv:physics/0503191](https://arxiv.org/abs/physics/0503191).
- [21] Particle Data Group, J. Beringer *et al.*, *Review of particle physics*, Phys. Rev. **D86** (2012) 010001, and 2013 partial update for the 2014 edition.
- [22] LHCb collaboration, R. Aaij *et al.*, *Measurements of the branching fractions of $B^+ \rightarrow p\bar{p}K^+$ decays*, Eur. Phys. J. **C73** (2013) 2462, [arXiv:1303.7133](https://arxiv.org/abs/1303.7133).
- [23] Belle collaboration, J.-T. Wei *et al.*, *Study of the decay mechanism for $B^+ \rightarrow p\bar{p}K^+$ and $B^+ \rightarrow p\bar{p}\pi^+$* , Phys. Lett. B **659** (2008) 80, [arXiv:0706.4167](https://arxiv.org/abs/0706.4167).
- [24] M. Suzuki, *Partial waves of baryon-antibaryon in three-body B meson decay*, J. Phys. **G34** (2007) 283, [arXiv:hep-ph/0609133](https://arxiv.org/abs/hep-ph/0609133).
- [25] F. W. Wieland *et al.*, *Study of the reaction $\gamma p \rightarrow K^+\Lambda(1520)$ at photon energies up to 2.65 GeV*, Eur. Phys. J. **A47** (2011) 47, erratum *ibid.* **A47** (2011) 133, [arXiv:1011.0822](https://arxiv.org/abs/1011.0822).

- [26] D0 collaboration, V. M. Abazov *et al.*, *Measurement of direct CP violation parameters in $B^\pm \rightarrow J/\psi K^\pm$ and $B^\pm \rightarrow J/\psi \pi^\pm$ decays with 10.4 fb^{-1} of Tevatron data*, Phys. Rev. Lett. **110** (2013) 241801, [arXiv:1304.1655](https://arxiv.org/abs/1304.1655).
- [27] LHCb collaboration, R. Aaij *et al.*, *Measurement of CP asymmetry in $D^0 \rightarrow K^- K^+$ and $D^0 \rightarrow \pi^- \pi^+$ decays*, JHEP **07** (2014) 041, [arXiv:1405.2797](https://arxiv.org/abs/1405.2797).

LHCb collaboration

R. Aaij⁴¹, B. Adeva³⁷, M. Adinolfi⁴⁶, A. Affolder⁵², Z. Ajaltouni⁵, S. Akar⁶, J. Albrecht⁹, F. Alessio³⁸, M. Alexander⁵¹, S. Ali⁴¹, G. Alkhazov³⁰, P. Alvarez Cartelle³⁷, A.A. Alves Jr^{25,38}, S. Amato², S. Amerio²², Y. Amhis⁷, L. An³, L. Anderlini^{17,g}, J. Anderson⁴⁰, R. Andreassen⁵⁷, M. Andreotti^{16,f}, J.E. Andrews⁵⁸, R.B. Appleby⁵⁴, O. Aquines Gutierrez¹⁰, F. Archilli³⁸, A. Artamonov³⁵, M. Artuso⁵⁹, E. Aslanides⁶, G. Auriemma^{25,n}, M. Baalouch⁵, S. Bachmann¹¹, J.J. Back⁴⁸, A. Badalov³⁶, W. Baldini¹⁶, R.J. Barlow⁵⁴, C. Barschel³⁸, S. Barsuk⁷, W. Barter⁴⁷, V. Batozskaya²⁸, V. Battista³⁹, A. Bay³⁹, L. Beaucourt⁴, J. Beddow⁵¹, F. Bedeschi²³, I. Bediaga¹, S. Belogurov³¹, K. Belous³⁵, I. Belyaev³¹, E. Ben-Haim⁸, G. Bencivenni¹⁸, S. Benson³⁸, J. Benton⁴⁶, A. Berezhnoy³², R. Bernet⁴⁰, M.-O. Bettler⁴⁷, M. van Beuzekom⁴¹, A. Bien¹¹, S. Bifani⁴⁵, T. Bird⁵⁴, A. Bizzeti^{17,i}, P.M. Bjørnstad⁵⁴, T. Blake⁴⁸, F. Blanc³⁹, J. Blouw¹⁰, S. Blusk⁵⁹, V. Bocci²⁵, A. Bondar³⁴, N. Bondar^{30,38}, W. Bonivento^{15,38}, S. Borghi⁵⁴, A. Borgia⁵⁹, M. Borsato⁷, T.J.V. Bowcock⁵², E. Bowen⁴⁰, C. Bozzi¹⁶, T. Brambach⁹, J. van den Brand⁴², J. Bressieux³⁹, D. Brett⁵⁴, M. Britsch¹⁰, T. Britton⁵⁹, J. Brodzicka⁵⁴, N.H. Brook⁴⁶, H. Brown⁵², A. Bursche⁴⁰, G. Busetto^{22,r}, J. Buytaert³⁸, S. Cadeddu¹⁵, R. Calabrese^{16,f}, M. Calvi^{20,k}, M. Calvo Gomez^{36,p}, P. Campana^{18,38}, D. Campora Perez³⁸, A. Carbone^{14,d}, G. Carboni^{24,l}, R. Cardinale^{19,38,j}, A. Cardini¹⁵, L. Carson⁵⁰, K. Carvalho Akiba², G. Casse⁵², L. Cassina²⁰, L. Castillo Garcia³⁸, M. Cattaneo³⁸, Ch. Cauet⁹, R. Cenci⁵⁸, M. Charles⁸, Ph. Charpentier³⁸, M. Chefdeville⁴, S. Chen⁵⁴, S.-F. Cheung⁵⁵, N. Chiapolini⁴⁰, M. Chrzaszcz^{40,26}, K. Ciba³⁸, X. Cid Vidal³⁸, G. Ciezarek⁵³, P.E.L. Clarke⁵⁰, M. Clemencic³⁸, H.V. Cliff⁴⁷, J. Closier³⁸, V. Coco³⁸, J. Cogan⁶, E. Cogneras⁵, P. Collins³⁸, A. Comerma-Montells¹¹, A. Contu¹⁵, A. Cook⁴⁶, M. Coombes⁴⁶, S. Coquereau⁸, G. Corti³⁸, M. Corvo^{16,f}, I. Counts⁵⁶, B. Couturier³⁸, G.A. Cowan⁵⁰, D.C. Craik⁴⁸, M. Cruz Torres⁶⁰, S. Cunliffe⁵³, R. Currie⁵⁰, C. D'Ambrosio³⁸, J. Dalseno⁴⁶, P. David⁸, P.N.Y. David⁴¹, A. Davis⁵⁷, K. De Bruyn⁴¹, S. De Capua⁵⁴, M. De Cian¹¹, J.M. De Miranda¹, L. De Paula², W. De Silva⁵⁷, P. De Simone¹⁸, D. Decamp⁴, M. Deckenhoff⁹, L. Del Buono⁸, N. Déléage⁴, D. Derkach⁵⁵, O. Deschamps⁵, F. Dettori³⁸, A. Di Canto³⁸, H. Dijkstra³⁸, S. Donleavy⁵², F. Dordei¹¹, M. Dorigo³⁹, A. Dosil Suárez³⁷, D. Dossett⁴⁸, A. Dovbnya⁴³, K. Dreimanis⁵², G. Dujany⁵⁴, F. Dupertuis³⁹, P. Durante³⁸, R. Dzhelyadin³⁵, A. Dziurda²⁶, A. Dzyuba³⁰, S. Easo^{49,38}, U. Egede⁵³, V. Egorychev³¹, S. Eidelman³⁴, S. Eisenhardt⁵⁰, U. Eitschberger⁹, R. Ekelhof⁹, L. Eklund⁵¹, I. El Rifai⁵, Ch. Elsasser⁴⁰, S. Ely⁵⁹, S. Esen¹¹, H.-M. Evans⁴⁷, T. Evans⁵⁵, A. Falabella¹⁴, C. Färber¹¹, C. Farinelli⁴¹, N. Farley⁴⁵, S. Farry⁵², RF Fay⁵², D. Ferguson⁵⁰, V. Fernandez Albor³⁷, F. Ferreira Rodrigues¹, M. Ferro-Luzzi³⁸, S. Filippov³³, M. Fiore^{16,f}, M. Fiorini^{16,f}, M. Firlej²⁷, C. Fitzpatrick³⁹, T. Fiutowski²⁷, M. Fontana¹⁰, F. Fontanelli^{19,j}, R. Forty³⁸, O. Francisco², M. Frank³⁸, C. Frei³⁸, M. Frosini^{17,38,g}, J. Fu^{21,38}, E. Furfarò^{24,l}, A. Gallas Torreira³⁷, D. Galli^{14,d}, S. Gallorini²², S. Gambetta^{19,j}, M. Gandelman², P. Gandini⁵⁹, Y. Gao³, J. García Pardiñas³⁷, J. Garofoli⁵⁹, J. Garra Tico⁴⁷, L. Garrido³⁶, C. Gaspar³⁸, R. Gauld⁵⁵, L. Gavardi⁹, G. Gavrilov³⁰, E. Gersabeck¹¹, M. Gersabeck⁵⁴, T. Gershon⁴⁸, Ph. Ghez⁴, A. Gianelle²², S. Giani³⁹, V. Gibson⁴⁷, L. Giubega²⁹, V.V. Gligorov³⁸, C. Göbel⁶⁰, D. Golubkov³¹, A. Golutvin^{53,31,38}, A. Gomes^{1,a}, C. Gotti²⁰, M. Grabalosa Gándara⁵, R. Graciani Diaz³⁶, L.A. Granado Cardoso³⁸, E. Graugés³⁶, G. Graziani¹⁷, A. Grecu²⁹, E. Greening⁵⁵, S. Gregson⁴⁷, P. Griffith⁴⁵, L. Grillo¹¹, O. Grünberg⁶², B. Gui⁵⁹, E. Gushchin³³, Yu. Guz^{35,38}, T. Gys³⁸, C. Hadjivasiliou⁵⁹, G. Haefeli³⁹, C. Haen³⁸, S.C. Haines⁴⁷, S. Hall⁵³, B. Hamilton⁵⁸, T. Hampson⁴⁶, X. Han¹¹, S. Hansmann-Menzemer¹¹, N. Harnew⁵⁵, S.T. Harnew⁴⁶, J. Harrison⁵⁴, J. He³⁸, T. Head³⁸, V. Heijne⁴¹, K. Hennessy⁵², P. Henrard⁵,

L. Henry⁸, J.A. Hernando Morata³⁷, E. van Herwijnen³⁸, M. Heß⁶², A. Hicheur¹, D. Hill⁵⁵,
 M. Hoballah⁵, C. Hombach⁵⁴, W. Hulsbergen⁴¹, P. Hunt⁵⁵, N. Hussain⁵⁵, D. Hutchcroft⁵²,
 D. Hynds⁵¹, M. Idzik²⁷, P. Ilten⁵⁶, R. Jacobsson³⁸, A. Jaeger¹¹, J. Jalocha⁵⁵, E. Jans⁴¹,
 P. Jaton³⁹, A. Jawahery⁵⁸, F. Jing³, M. John⁵⁵, D. Johnson⁵⁵, C.R. Jones⁴⁷, C. Joram³⁸,
 B. Jost³⁸, N. Jurik⁵⁹, M. Kaballo⁹, S. Kandybei⁴³, W. Kanso⁶, M. Karacson³⁸, T.M. Karbach³⁸,
 S. Karodia⁵¹, M. Kelsey⁵⁹, I.R. Kenyon⁴⁵, T. Ketel⁴², B. Khanji²⁰, C. Khurewathanakul³⁹,
 S. Klaver⁵⁴, K. Klimaszewski²⁸, O. Kochebina⁷, M. Kolpin¹¹, I. Komarov³⁹, R.F. Koopman⁴²,
 P. Koppenburg^{41,38}, M. Korolev³², A. Kozlinskiy⁴¹, L. Kravchuk³³, K. Kreplin¹¹, M. Kreps⁴⁸,
 G. Krocker¹¹, P. Krokovny³⁴, F. Kruse⁹, W. Kucewicz^{26,o}, M. Kucharczyk^{20,26,38,k},
 V. Kudryavtsev³⁴, K. Kurek²⁸, T. Kvaratskheliya³¹, V.N. La Thi³⁹, D. Lacarrere³⁸,
 G. Lafferty⁵⁴, A. Lai¹⁵, D. Lambert⁵⁰, R.W. Lambert⁴², G. Lanfranchi¹⁸, C. Langenbruch⁴⁸,
 B. Langhans³⁸, T. Latham⁴⁸, C. Lazzeroni⁴⁵, R. Le Gac⁶, J. van Leerdam⁴¹, J.-P. Lees⁴,
 R. Lefèvre⁵, A. Leflat³², J. Lefrançois⁷, S. Leo²³, O. Leroy⁶, T. Lesiak²⁶, B. Leverington¹¹,
 Y. Li³, T. Likhomanenko⁶³, M. Liles⁵², R. Lindner³⁸, C. Linn³⁸, F. Lionetto⁴⁰, B. Liu¹⁵,
 S. Lohn³⁸, I. Longstaff⁵¹, J.H. Lopes², N. Lopez-March³⁹, P. Lowdon⁴⁰, H. Lu³, D. Lucchesi^{22,r},
 H. Luo⁵⁰, A. Lupato²², E. Luppi^{16,f}, O. Lupton⁵⁵, F. Machefert⁷, I.V. Machikhiliyan³¹,
 F. Maciuc²⁹, O. Maev³⁰, S. Malde⁵⁵, A. Malinin⁶³, G. Manca^{15,e}, G. Mancinelli⁶, J. Maratas⁵,
 J.F. Marchand⁴, U. Marconi¹⁴, C. Marin Benito³⁶, P. Marino^{23,t}, R. Märki³⁹, J. Marks¹¹,
 G. Martellotti²⁵, A. Martens⁸, A. Martín Sánchez⁷, M. Martinelli⁴¹, D. Martinez Santos⁴²,
 F. Martinez Vidal⁶⁴, D. Martins Tostes², A. Massafferri¹, R. Matev³⁸, Z. Mathe³⁸,
 C. Matteuzzi²⁰, A. Mazurov^{16,f}, M. McCann⁵³, J. McCarthy⁴⁵, A. McNab⁵⁴, R. McNulty¹²,
 B. McSkelly⁵², B. Meadows⁵⁷, F. Meier⁹, M. Meissner¹¹, M. Merk⁴¹, D.A. Milanes⁸,
 M.-N. Minard⁴, N. Moggi¹⁴, J. Molina Rodriguez⁶⁰, S. Monteil⁵, M. Morandin²², P. Morawski²⁷,
 A. Mordà⁶, M.J. Morello^{23,t}, J. Moron²⁷, A.-B. Morris⁵⁰, R. Mountain⁵⁹, F. Muheim⁵⁰,
 K. Müller⁴⁰, M. Mussini¹⁴, B. Muster³⁹, P. Naik⁴⁶, T. Nakada³⁹, R. Nandakumar⁴⁹, I. Nasteva²,
 M. Needham⁵⁰, N. Neri²¹, S. Neubert³⁸, N. Neufeld³⁸, M. Neuner¹¹, A.D. Nguyen³⁹,
 T.D. Nguyen³⁹, C. Nguyen-Mau^{39,q}, M. Nicol⁷, V. Niess⁵, R. Niet⁹, N. Nikitin³², T. Nikodem¹¹,
 A. Novoselov³⁵, D.P. O'Hanlon⁴⁸, A. Oblakowska-Mucha²⁷, V. Obraztsov³⁵, S. Oggero⁴¹,
 S. Ogilvy⁵¹, O. Okhrimenko⁴⁴, R. Oldeman^{15,e}, G. Onderwater⁶⁵, M. Orlandea²⁹,
 J.M. Otalora Goicochea², P. Owen⁵³, A. Oyanguren⁶⁴, B.K. Pal⁵⁹, A. Palano^{13,c}, F. Palombo^{21,u},
 M. Palutan¹⁸, J. Panman³⁸, A. Papanestis^{49,38}, M. Pappagallo⁵¹, L.L. Pappalardo^{16,f},
 C. Parkes⁵⁴, C.J. Parkinson^{9,45}, G. Passaleva¹⁷, G.D. Patel⁵², M. Patel⁵³, C. Patrignani^{19,j},
 A. Pazos Alvarez³⁷, A. Pearce⁵⁴, A. Pellegrino⁴¹, M. Pepe Altarelli³⁸, S. Perazzini^{14,d},
 E. Perez Trigo³⁷, P. Perret⁵, M. Perrin-Terrin⁶, L. Pescatore⁴⁵, E. Pesen⁶⁶, K. Petridis⁵³,
 A. Petrolini^{19,j}, E. Picatoste Olloqui³⁶, B. Pietrzyk⁴, T. Pilař⁴⁸, D. Pinci²⁵, A. Pistone¹⁹,
 S. Playfer⁵⁰, M. Plo Casasus³⁷, F. Polci⁸, A. Poluektov^{48,34}, E. Polycarpo², A. Popov³⁵,
 D. Popov¹⁰, B. Popovici²⁹, C. Potterat², E. Price⁴⁶, J. Prisciandaro³⁹, A. Pritchard⁵²,
 C. Prouve⁴⁶, V. Pugatch⁴⁴, A. Puig Navarro³⁹, G. Punzi^{23,s}, W. Qian⁴, B. Rachwal²⁶,
 J.H. Rademacker⁴⁶, B. Rakotomiaramanana³⁹, M. Rama¹⁸, M.S. Rangel², I. Raniuk⁴³,
 N. Rauschmayr³⁸, G. Raven⁴², S. Reichert⁵⁴, M.M. Reid⁴⁸, A.C. dos Reis¹, S. Ricciardi⁴⁹,
 S. Richards⁴⁶, M. Rihl³⁸, K. Rinnert⁵², V. Rives Molina³⁶, D.A. Roa Romero⁵, P. Robbe⁷,
 A.B. Rodrigues¹, E. Rodrigues⁵⁴, P. Rodriguez Perez⁵⁴, S. Roiser³⁸, V. Romanovsky³⁵,
 A. Romero Vidal³⁷, M. Rotondo²², J. Rouvinet³⁹, T. Ruf³⁸, F. Ruffini²³, H. Ruiz³⁶,
 P. Ruiz Valls⁶⁴, J.J. Saborido Silva³⁷, N. Sagidova³⁰, P. Sail⁵¹, B. Saitta^{15,e},
 V. Salustino Guimaraes², C. Sanchez Mayordomo⁶⁴, B. Sanmartin Sedes³⁷, R. Santacesaria²⁵,
 C. Santamarina Rios³⁷, E. Santovetti^{24,l}, A. Sarti^{18,m}, C. Satriano^{25,n}, A. Satta²⁴,

D.M. Saunders⁴⁶, M. Savrie^{16,f}, D. Savrina^{31,32}, M. Schiller⁴², H. Schindler³⁸, M. Schlupp⁹, M. Schmelling¹⁰, B. Schmidt³⁸, O. Schneider³⁹, A. Schopper³⁸, M.-H. Schune⁷, R. Schwemmer³⁸, B. Sciascia¹⁸, A. Sciubba²⁵, M. Seco³⁷, A. Semennikov³¹, I. Sepp⁵³, N. Serra⁴⁰, J. Serrano⁶, L. Sestini²², P. Seyfert¹¹, M. Shapkin³⁵, I. Shapoval^{16,43,f}, Y. Shcheglov³⁰, T. Shears⁵², L. Shekhtman³⁴, V. Shevchenko⁶³, A. Shires⁹, R. Silva Coutinho⁴⁸, G. Simi²², M. Sirendi⁴⁷, N. Skidmore⁴⁶, T. Skwarnicki⁵⁹, N.A. Smith⁵², E. Smith^{55,49}, E. Smith⁵³, J. Smith⁴⁷, M. Smith⁵⁴, H. Snoek⁴¹, M.D. Sokoloff⁵⁷, F.J.P. Soler⁵¹, F. Soomro³⁹, D. Souza⁴⁶, B. Souza De Paula², B. Spaan⁹, A. Sparkes⁵⁰, P. Spradlin⁵¹, S. Sridharan³⁸, F. Stagni³⁸, M. Stahl¹¹, S. Stahl¹¹, O. Steinkamp⁴⁰, O. Stenyakin³⁵, S. Stevenson⁵⁵, S. Stoica²⁹, S. Stone⁵⁹, B. Storaci⁴⁰, S. Stracka^{23,38}, M. Straticiuc²⁹, U. Straumann⁴⁰, R. Stroili²², V.K. Subbiah³⁸, L. Sun⁵⁷, W. Sutcliffe⁵³, K. Swientek²⁷, S. Swientek⁹, V. Syropoulos⁴², M. Szczekowski²⁸, P. Szczypka^{39,38}, D. Szilard², T. Szumlak²⁷, S. T'Jampens⁴, M. Teklishyn⁷, G. Tellarini^{16,f}, F. Teubert³⁸, C. Thomas⁵⁵, E. Thomas³⁸, J. van Tilburg⁴¹, V. Tisserand⁴, M. Tobin³⁹, S. Tolk⁴², L. Tomassetti^{16,f}, D. Tonelli³⁸, S. Topp-Joergensen⁵⁵, N. Torr⁵⁵, E. Tournefier⁴, S. Tourneur³⁹, M.T. Tran³⁹, M. Tresch⁴⁰, A. Tsaregorodtsev⁶, P. Tsopelas⁴¹, N. Tuning⁴¹, M. Ubeda Garcia³⁸, A. Ukleja²⁸, A. Ustyuzhanin⁶³, U. Uwer¹¹, V. Vagnoni¹⁴, G. Valenti¹⁴, A. Vallier⁷, R. Vazquez Gomez¹⁸, P. Vazquez Regueiro³⁷, C. Vázquez Sierra³⁷, S. Vecchi¹⁶, J.J. Velthuis⁴⁶, M. Veltri^{17,h}, G. Veneziano³⁹, M. Vesterinen¹¹, B. Viaud⁷, D. Vieira², M. Vieites Diaz³⁷, X. Vilasis-Cardona^{36,p}, A. Vollhardt⁴⁰, D. Volyansky¹⁰, D. Voong⁴⁶, A. Vorobyev³⁰, V. Vorobyev³⁴, C. Voß⁶², H. Voss¹⁰, J.A. de Vries⁴¹, R. Waldi⁶², C. Wallace⁴⁸, R. Wallace¹², J. Walsh²³, S. Wandernoth¹¹, J. Wang⁵⁹, D.R. Ward⁴⁷, N.K. Watson⁴⁵, D. Websdale⁵³, M. Whitehead⁴⁸, J. Wicht³⁸, D. Wiedner¹¹, G. Wilkinson⁵⁵, M.P. Williams⁴⁵, M. Williams⁵⁶, F.F. Wilson⁴⁹, J. Wimberley⁵⁸, J. Wishahi⁹, W. Wislicki²⁸, M. Witek²⁶, G. Wormser⁷, S.A. Wotton⁴⁷, S. Wright⁴⁷, S. Wu³, K. Wyllie³⁸, Y. Xie⁶¹, Z. Xing⁵⁹, Z. Xu³⁹, Z. Yang³, X. Yuan³, O. Yushchenko³⁵, M. Zangoli¹⁴, M. Zavertyaev^{10,b}, L. Zhang⁵⁹, W.C. Zhang¹², Y. Zhang³, A. Zhelezov¹¹, A. Zhokhov³¹, L. Zhong³, A. Zvyagin³⁸.

¹Centro Brasileiro de Pesquisas Físicas (CBPF), Rio de Janeiro, Brazil

²Universidade Federal do Rio de Janeiro (UFRJ), Rio de Janeiro, Brazil

³Center for High Energy Physics, Tsinghua University, Beijing, China

⁴LAPP, Université de Savoie, CNRS/IN2P3, Annecy-Le-Vieux, France

⁵Clermont Université, Université Blaise Pascal, CNRS/IN2P3, LPC, Clermont-Ferrand, France

⁶CPPM, Aix-Marseille Université, CNRS/IN2P3, Marseille, France

⁷LAL, Université Paris-Sud, CNRS/IN2P3, Orsay, France

⁸LPNHE, Université Pierre et Marie Curie, Université Paris Diderot, CNRS/IN2P3, Paris, France

⁹Fakultät Physik, Technische Universität Dortmund, Dortmund, Germany

¹⁰Max-Planck-Institut für Kernphysik (MPIK), Heidelberg, Germany

¹¹Physikalisches Institut, Ruprecht-Karls-Universität Heidelberg, Heidelberg, Germany

¹²School of Physics, University College Dublin, Dublin, Ireland

¹³Sezione INFN di Bari, Bari, Italy

¹⁴Sezione INFN di Bologna, Bologna, Italy

¹⁵Sezione INFN di Cagliari, Cagliari, Italy

¹⁶Sezione INFN di Ferrara, Ferrara, Italy

¹⁷Sezione INFN di Firenze, Firenze, Italy

¹⁸Laboratori Nazionali dell'INFN di Frascati, Frascati, Italy

¹⁹Sezione INFN di Genova, Genova, Italy

²⁰Sezione INFN di Milano Bicocca, Milano, Italy

²¹Sezione INFN di Milano, Milano, Italy

²²Sezione INFN di Padova, Padova, Italy

- ²³Sezione INFN di Pisa, Pisa, Italy
²⁴Sezione INFN di Roma Tor Vergata, Roma, Italy
²⁵Sezione INFN di Roma La Sapienza, Roma, Italy
²⁶Henryk Niewodniczanski Institute of Nuclear Physics Polish Academy of Sciences, Kraków, Poland
²⁷AGH - University of Science and Technology, Faculty of Physics and Applied Computer Science, Kraków, Poland
²⁸National Center for Nuclear Research (NCBJ), Warsaw, Poland
²⁹Horia Hulubei National Institute of Physics and Nuclear Engineering, Bucharest-Magurele, Romania
³⁰Petersburg Nuclear Physics Institute (PNPI), Gatchina, Russia
³¹Institute of Theoretical and Experimental Physics (ITEP), Moscow, Russia
³²Institute of Nuclear Physics, Moscow State University (SINP MSU), Moscow, Russia
³³Institute for Nuclear Research of the Russian Academy of Sciences (INR RAN), Moscow, Russia
³⁴Budker Institute of Nuclear Physics (SB RAS) and Novosibirsk State University, Novosibirsk, Russia
³⁵Institute for High Energy Physics (IHEP), Protvino, Russia
³⁶Universitat de Barcelona, Barcelona, Spain
³⁷Universidad de Santiago de Compostela, Santiago de Compostela, Spain
³⁸European Organization for Nuclear Research (CERN), Geneva, Switzerland
³⁹Ecole Polytechnique Fédérale de Lausanne (EPFL), Lausanne, Switzerland
⁴⁰Physik-Institut, Universität Zürich, Zürich, Switzerland
⁴¹Nikhef National Institute for Subatomic Physics, Amsterdam, The Netherlands
⁴²Nikhef National Institute for Subatomic Physics and VU University Amsterdam, Amsterdam, The Netherlands
⁴³NSC Kharkiv Institute of Physics and Technology (NSC KIPT), Kharkiv, Ukraine
⁴⁴Institute for Nuclear Research of the National Academy of Sciences (KINR), Kyiv, Ukraine
⁴⁵University of Birmingham, Birmingham, United Kingdom
⁴⁶H.H. Wills Physics Laboratory, University of Bristol, Bristol, United Kingdom
⁴⁷Cavendish Laboratory, University of Cambridge, Cambridge, United Kingdom
⁴⁸Department of Physics, University of Warwick, Coventry, United Kingdom
⁴⁹STFC Rutherford Appleton Laboratory, Didcot, United Kingdom
⁵⁰School of Physics and Astronomy, University of Edinburgh, Edinburgh, United Kingdom
⁵¹School of Physics and Astronomy, University of Glasgow, Glasgow, United Kingdom
⁵²Oliver Lodge Laboratory, University of Liverpool, Liverpool, United Kingdom
⁵³Imperial College London, London, United Kingdom
⁵⁴School of Physics and Astronomy, University of Manchester, Manchester, United Kingdom
⁵⁵Department of Physics, University of Oxford, Oxford, United Kingdom
⁵⁶Massachusetts Institute of Technology, Cambridge, MA, United States
⁵⁷University of Cincinnati, Cincinnati, OH, United States
⁵⁸University of Maryland, College Park, MD, United States
⁵⁹Syracuse University, Syracuse, NY, United States
⁶⁰Pontifícia Universidade Católica do Rio de Janeiro (PUC-Rio), Rio de Janeiro, Brazil, associated to ²
⁶¹Institute of Particle Physics, Central China Normal University, Wuhan, Hubei, China, associated to ³
⁶²Institut für Physik, Universität Rostock, Rostock, Germany, associated to ¹¹
⁶³National Research Centre Kurchatov Institute, Moscow, Russia, associated to ³¹
⁶⁴Instituto de Fisica Corpuscular (IFIC), Universitat de Valencia-CSIC, Valencia, Spain, associated to ³⁶
⁶⁵KVI - University of Groningen, Groningen, The Netherlands, associated to ⁴¹
⁶⁶Celal Bayar University, Manisa, Turkey, associated to ³⁸

^aUniversidade Federal do Triângulo Mineiro (UFTM), Uberaba-MG, Brazil

^bP.N. Lebedev Physical Institute, Russian Academy of Science (LPI RAS), Moscow, Russia

^cUniversità di Bari, Bari, Italy

^dUniversità di Bologna, Bologna, Italy

^eUniversità di Cagliari, Cagliari, Italy

- ^f Università di Ferrara, Ferrara, Italy
^g Università di Firenze, Firenze, Italy
^h Università di Urbino, Urbino, Italy
ⁱ Università di Modena e Reggio Emilia, Modena, Italy
^j Università di Genova, Genova, Italy
^k Università di Milano Bicocca, Milano, Italy
^l Università di Roma Tor Vergata, Roma, Italy
^m Università di Roma La Sapienza, Roma, Italy
ⁿ Università della Basilicata, Potenza, Italy
^o AGH - University of Science and Technology, Faculty of Computer Science, Electronics and Telecommunications, Kraków, Poland
^p LIFAELS, La Salle, Universitat Ramon Llull, Barcelona, Spain
^q Hanoi University of Science, Hanoi, Viet Nam
^r Università di Padova, Padova, Italy
^s Università di Pisa, Pisa, Italy
^t Scuola Normale Superiore, Pisa, Italy
^u Università degli Studi di Milano, Milano, Italy